Mapping of hyperthermic tumor cell death in a microchannel under unidirectional heating

Fen Wang, Yuhui Li, Lei Chen, Dandan Chen, Xiaolei Wu,[a] and Hao Wang[a]
College of Engineering, Peking University, Beijing, China

(Received 15 December 2011; accepted 26 February 2012; published online 20 March 2012)

Hyperthermia can be used as an adjunctive method of chemotherapy, radiotherapy, and gene therapy to improve cancer treatment. In this study, we investigate the hyperthermic cell death of cervix cancer CaSki cells in a microchannel integrated with a directional heating scheme. Heat was applied from the inner end to the outer end of the channel and a temperature distribution from 60 °C to 30 °C was established. A three dimensional (3D) numerical model was conducted for the heat transfer simulation, based on which a simple fitting method was proposed to easily estimate the temperature distribution along the channel. Cell death along the channel was mapped 22 h after the heating treatment by dual fluorescent labeling and phase-contrast microscopy imaging. Upstream, where the temperature is higher than 42 °C, we observe necrotic death, late-stage and early stage apoptotic death in sequence along the channel. Downstream and in the middle of the channel, where the temperature is lower than 42 °C, significant cell detachment was noted. Vigorous detachment was observed even in the non-hyperthermic zone (temperature lower than 37 °C), which we believe is due to the direct effect of the hyperthermic zones (higher than 37 °C). The present work not only gives a vivid map of cell responses under a temperature gradient, but also reveals the potential interactions of the heated tumor cells and non-heated tumor cells, which are seldom investigated in conventional petri-dish experiments. © *2012 American Institute of Physics*.
[http://dx.doi.org/10.1063/1.3694252]

I. INTRODUCTION

In the past few years, hyperthermia has gained a lot of interest as an effective adjunctive method of chemotherapy, radiotherapy, and gene therapy[1–4] in cancer treatments. Successful hyperthermic treatments rely on the balance between killing the majority of cancerous cells, while protecting the healthy cells when the tumorous tissues are exposed to high temperatures. It is of great importance to identify the associated damage to both the cancer cells and the neighboring healthy tissues. There is extensive research in this particular field, both *in vivo*[5–7] and *in vitro*,[8–11] but numerous challenges remain due to the complex physical and physiological properties and variety of tissues.

Cell damage caused by hyperthermia has been studied for a few decades. Vidair *et al.*[12] proposed two distinct modes of hyperthermic cell death based on time tracking. A "rapid" mode was characterized by cell detachment and inhibited rates of macromolecular synthesis, which usually dominates during the first few days post heating. A "slow" mode was defined to describe the processes after the cells had fully recovered from the heat-induced inhibition of macromolecular synthesis, and cell detachment had ceased. Roti *et al.*[13] reviewed the mechanisms of hyperthermic induced cell killing at the cellular level. Hyperthermia not only has effects on the plasma membrane protein distribution which related with calcium spike, disrupts mitochondrial membrane potential resulting in the redox status of the cells, but also has significant impacts on the nucleus such as double strand break. Recent research by Shellman *et al.*[14] indicated that hyperthermia can also induce endoplasmic reticulum mediated apoptosis. Hyperthermia can induce necrotic and apoptotic cell death

[a]Authors to whom correspondence should be addressed. Electronic addresses: xiaolei_wu@pku.edu.cn and hwang@coe.pku.edu.cn.

depending on the temperature distribution and time spans. Harmon *et al.*[15] categorized the death occurring after various heat loads and distinguished the necrosis and apoptosis by the extent of membrane disruption or DNA damage. Moroi *et al.*[7] studied the regional dead-cell distribution by examining the necrosis and apoptosis in the center and periphery of the solid nodules of gliosarcoma (T9) in vivo by heating for 30 min in a water bath at 43 °C. They found necrosis was enhanced in 3∼6 h post heating, while a regional difference in the rate of apoptosis was detected immediately after heating. Apoptosis can induce a group of proteins named HSPs (heat shock proteins) which will trigger thermotolerance and protect cells from heat-induced apoptosis.[16–18] Even though necrosis and apoptosis have been observed and differentiated in a variety of heating experiments, their sensitivity to temperature in vivo or in vitro and their development might be better interpreted either experimentally or theoretically.

The main drawbacks in the previous in vitro experiments is that the heating was performed in either a dedicated water bath or a heating stage,[15,19] where the temperature in the test section is approximately uniform. However, in practice, uniformly high temperature is hard to achieve in living systems due to the diverse physical thermal conductivity of organs, tissues, and blood flow, especially in cases when an external heat source, such as a heating probe, is applied. Extensive research of temperature-gradient control has been conducted in PCR for DNA amplification in a microfluidic platform,[20–22] but very few studies have been conducted to investigate temperature-gradient effects on cells. Das *et al.*[23] designed a microfluidic thermal gradient system in an incubator environment and showed its potential in thermotaxis studies. Lucchetta *et al.*[24] used microfluidic laminar flow to create a temperature difference around a Drosophila embryo and observed the density difference of nuclei in the two halves of the embryo affected by a T-step. However, few studies have been conducted to investigate the cell responses under a unidirectional heating and the interactions of the heated cells and non-heated cells with a regional or selected hyperthermic treatment of some of the cells in a microfluidic environment.

The present work aims to study the hyperthermic death of CaSki cells seeded in a single PDMS (polydimethysiloxane) microfluidic channel with unidirectional heating along the channel length. The temperature system was easily controlled by a heating tungsten wire embedded in the PDMS mold. A mathematical model was proposed to calculate the temperature distribution along the channel. The cell damage and the trend of the cell responses were mapped along the channel by identifying the apoptosis/necrosis rates using a commercial apoptosis kit (Annexin V-FITC&PI). Moreover, the interactions between hyperthermic and non-hyperthermic zones were revealed.

II. MATERIALS AND METHODS

A. Microchip fabrication

Microfluidic devices were fabricated in PDMS using the standard soft lithography method and replica molding.[25] The detailed fabrication procedure was presented in our previous papers.[26,27] In short, microscale patterns of channels in the photomask were replicated photolithographically using a negative photoresist (Microchem, Newton, MA) in a 100 class clean room. The inlet and outlet reservoirs for cell loading or collecting were punched with a 3 mm aiguille. The holes for thermocouples were punched by a 20 gauge needle. The tungsten wire (200 μm diameter) was sandwiched between the PDMS slab and the cleaned 1 mm thick, 25×75 mm glass slides, which were sealed together by an oxygen plasma treatment (Plasma-Therm Etcher, Diener electronic Co. LTD, Germany). The wire was positioned near the inlet reservoir perpendicular to the channel. The PDMS chips and the heating wire were exposed to UV light for around four hours in a safety cabinet (MSC-Advantage, Thermo Fisher Scientific Inc., MA, USA) in order to sterilize them before each experiment.

B. Heating system and operation

Metal wires generate heat when an electric current is applied. In the present design, a piece of tungsten wire was used as the heating wire. It was fixed near the inlet reservoir at a distance

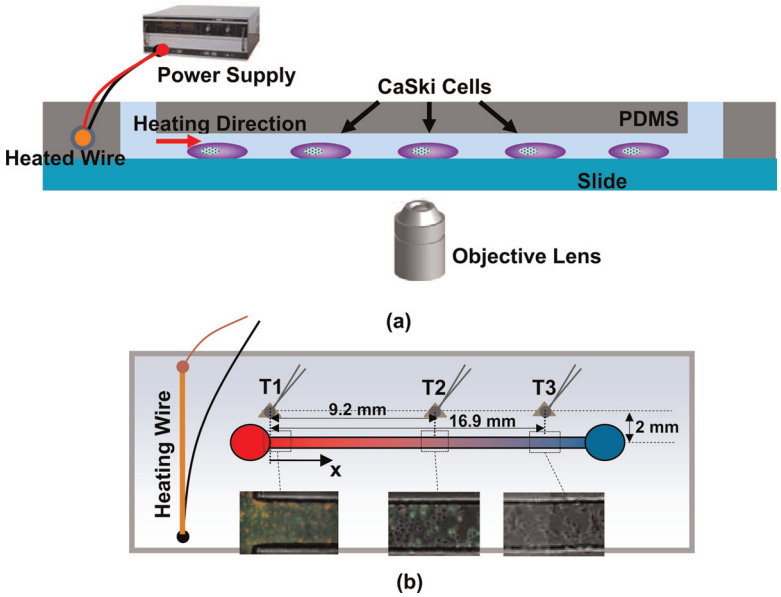

FIG. 1. Schematic diagram of the microchip integrated with a directional heating scheme: side view (a) and top view (b). The inserts are the fluorescent images of the cells on the first day post-heating located at the positions corresponding to each temperature measurement point.

of about 4.5 mm, perpendicular to the longitudinal direction of the channel (Fig. 1). Three K-type thermo couples, namely T1, T2, and T3, were embedded near the channel (2 mm away and parallel), 9200 μm and 16 900 μm away from the inlet, respectively. The temperatures were recorded through a data acquisition system (UTL/D-08LS1V0N, UTOP Electronic Co. LTD, Guangzhou, China). The power was supplied by a DC-stabilized source (WYK-5030, Huatai Electronics Co. LTD, Yangzhou, China). After the microchip was mounted on the clean microscopy stage, a voltage was applied to the heating wire to induce a local high temperature near the inlet and the temperature decreased along the microchannel. When the temperature distribution reached a steady state (which took around 15$\sim$20 min), the temperature at the inlet was $\approx$60 °C and $\approx$30 °C at the outlet. The heating lasted for 105 min (from the power being turned on) and then the power supply was disconnected. It took 5$\sim$10 min for the chip to cool down to room temperature.

C. General cell culture

Cervical cancer CaSki cell line was chosen in our study which is known to be sensitive to a combination of radiation and hyperthermia.[28] Cervical cancer CaSki cell line was cultured in plastic culture petri-dish at 37 °C, under 5% CO2 in Dulbecco's modified Eagle's medium (DMEM, Hyclone, Logan, UT) supplemented with 10% (v/v) fetal bovine serum (FBS, Hyclone, Logan, UT) and penicillin (100 units/ml, Hyclone, Logan, UT). CaSki cultures were maintained in 60 mm petri-dish (Corning) in a CO2 incubator (Forma Series II, Thermo Fisher Scientific Inc., MA, USA) at 37 °C and humidified atmosphere with 5% CO2. Cells were diluted at a ratio of 1:5 every 3 days to maintain them in the exponential growth phase ($\sim 1 \times 10^6$ cells/ml). Cells were harvested by adding 0.25% Trypsin-EDTA (Hyclone, Logan, UT) to the culture and centrifuged at 300 g for 10 min to remove the supernatant. The cells were then resuspended in the culture medium at a higher concentration before seeding in the microfluidic device.

D. Cell seeding and culture in the microchip

The channels were coated with fibronectin from bovine plasma (Sigma, St. Louis, MO) to facilitate cell adhesion. The activity of fibronectin remained unchanged up to 55 °C as observed

previously by Vuento *et al.*[29] Therefore, cell detachment by the denaturation of fibronectin could be eliminated in our experiment, if the temperature were lower than 55 °C. Fibronectin was prepared at a concentration of 50 μg/ml in phosphate-buffered saline (PBS) (Beijing Chemicals Co. LTD., China) before each experiment and then was introduced into the microfluidic device and incubated at 37 °C for 30 min. Prepared CaSki cells were suspended in the culture media, injected into the sample reservoirs of the microfluidic device, and allowed to spread and attach for 5–15 min. After adding extra culture media in both reservoirs, the device with seeded cells was incubated in a 37 °C, 5% CO2 incubator (Forma Series II, Thermo Fisher Scientific Inc., MA, USA) before hyperthermic experiments. Renewing the media in the reservoirs, every few hours provided enough media to support cell growth inside the device.

E. Sample treatment

To test the apoptosis and necrosis, a dual staining using an Annexin V-FITC/PI apoptosis detection kit (KeyGen Biotech. Co. LTD., Nanjing, China) was performed in a microfluidic cell culture system. Apoptotic cells translocate the membrane phosphatidylserine (PS) from the inner face of the plasma membrane to the outside which can be easily detected by staining with a fluorescent conjugate of Annexin V, which has a high affinity for PS. Propidium iodide (PI) is membrane-impenetrable and usually used to identify necrotic cells or late apoptotic cells whose membrane is not intact. With the combination of these two chemicals, it was possible for intact cells, initial apoptosis, middle or late apoptosis, and necrosis to be distinguished. The reagent was diluted by binding buffer to a final concentration suggested by the supplier. The culture medium was removed and the channel was washed twice with fresh PBS buffer. A drop of prepared reagent (around 50 μl) was added to the reservoir, and the culture channel was filled. The chip was incubated in the CO2 incubator at 37 °C for 10 min before testing the cell viability.

F. Fluorescence microscopy

Fluorescent and phase contrast images were taken on an inverted fluorescence microscopy (TI-U INVERTED, Nikon, Japan) with a CCD camera (Monochrome Cooled Digital Camera Head DS-Qi1Mc, Nikon, Japan). The setting of the CCD camera and the software were kept identical from one experiment to another whenever comparison between experiments was desired. In this experiment, Annexin V-FITC (465–495 nm) was excited by blue light and emitted green fluorescence, while propidium iodide (PI, 535/617 nm) was excited by green light and emitted red fluorescence.

III. RESULTS AND DISCUSSION

A. Directional heating

The growing cultured CaSki cells were exposed to the directional heating in the single microfluidic channel. The temperature profiles T1, T2, and T3 at three positions (at a distance of 0 μm, 9200 μm, and 16 900 μm from the inlet reservoir, respectively) were recorded. Under the heating power of about 0.47 W, T1, T2, and T3 reached a steady state of around 60±2 °C, 42±3 °C, and 33±2 °C, respectively, which are represented by the three triangle points marked in Fig. 2(a).

To have the temperature distribution along the channel, a 3D computational fluid dynamics (CFD) model is established to simulate the heat transfer of the system. The conduction in the chip, the heat dissipation on the chip surfaces, and the natural convection in the ambient air are all considered in the model. The material properties employed in the simulation are shown in Table I. Commercial software package FLUENT 6 is employed for the geometry setup and also the numerical treatment. As a result, the temperature distribution on the chip is obtained as shown in Fig. 2(b). The temperature distribution along the microchannel is extracted and shown by the dashed curve in Fig. 2(a). A good agreement is seen with the three experimental points.

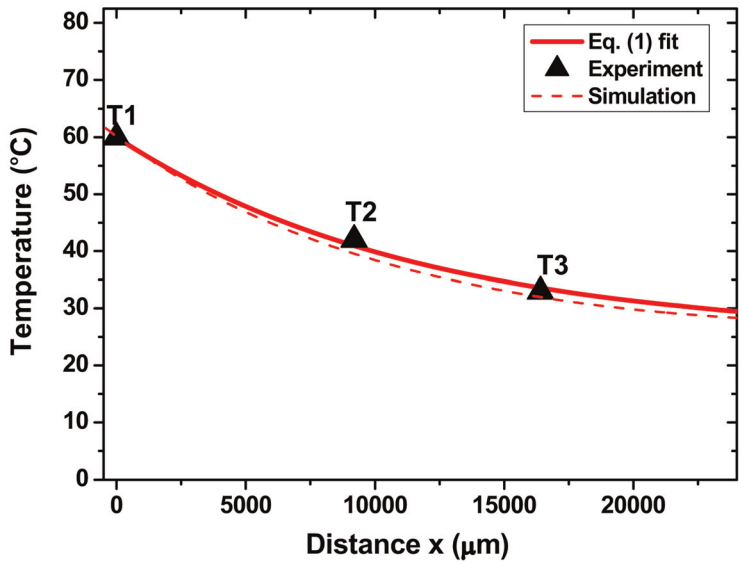

(a)

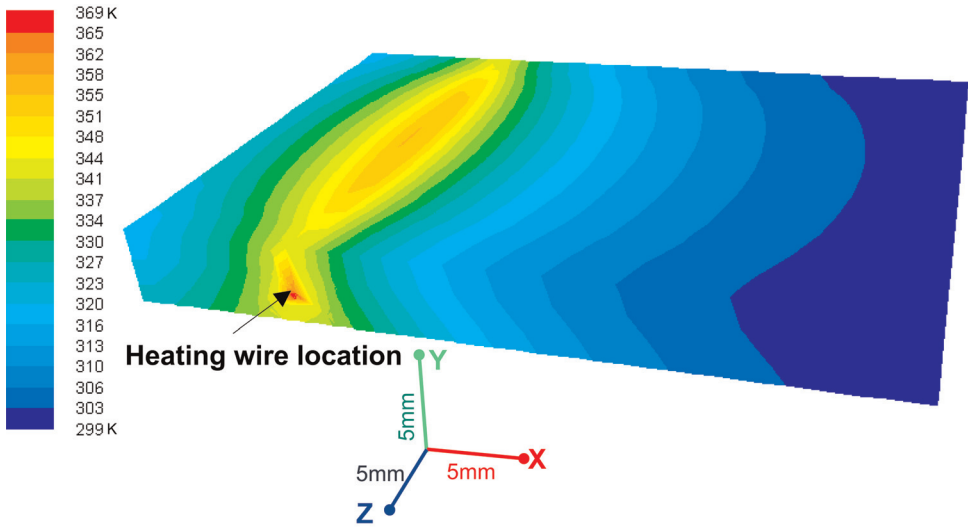

(b)

FIG. 2. Temperature along the chip: (a) temperatures at three locations measured by thermocouples (black triangle), the simulation result (dashed curve), and the fitting result based on fin theory (solid curve); (b) the simulated temperature distribution on the chip.

TABLE I. Material properties employed in simulation.

Properties	PDMS	Glass	Air
Density (kg/m^3)	1020	2500	Incompressible ideal gas
Thermal conductivity (W/m K)	0.18	1.4	0.0242
Thermal capacity (J/kg)	1460	840	1006.43
Viscosity (kg/m s)	—	—	1.789×10^{-5}

The chip temperature distribution in Fig. 2(b) indicates that the temperature change is mainly occurring along the x direction. Due to the simplicity of the present setup, the temperatures along the channel at the steady states can be easily obtained by making a fitting based on the heat transfer theories about a fin.[30] We justify this by noting that since the chip thickness (∼4 mm) is much smaller than the chip length (∼30 mm), the heat is dissipating into the air mainly on the top and bottom surfaces, and the chip can be treated like a fin. The temperature distribution in the fin along x direction is[30]

$$\theta = \theta_0 \frac{e^{mx} + e^{2mH} e^{-mx}}{1 + e^{2mH}}, \tag{1}$$

where θ is the excess temperature ($\theta = \mathrm{T} - \mathrm{Tair}$), θ_0 is the excess temperature at the fin base and H is the length of the fin. Based on this equation, a temperature curve along the channel can be fitted as shown in Fig. 2(b). This fitted curve will be employed in the following sections as the temperature distribution along the channel.

B. Maps of cell death under the temperature gradients

The cells were cultured for 22 h following heating treatment. A map of cell damage along the channel was then conducted by means of fluorescent staining and phase-contrast imaging. The results are combined and shown in Fig. 3(a). A control experiment was also conducted and no obvious change was detected except spontaneous apoptosis.

As introduced in Sec. III A, PI is membrane-impenetrable and usually used to identify necrotic cells or late apoptotic cells whose membrane is not intact. In Fig. 3(a), the red fluorescence represents the nuclei that were stained with PI. The dense red dots in the upstream of the channel from 0∼7000 μm (>45 °C) indicate vast necrosis or late-stage apoptosis in this area. Downstream along the channel, the proportion of the necrotic cells decreases and the proportion of apoptotic cells increases. The apoptotic cells at the early stage were stained by FITC in the membrane only (green fluorescence). Further downstream the cells were not stained by either PI or FITC, but their morphology alteration, such as rounding up, might indicate that they were undergoing apoptosis.

The cell morphology along the channel can also be used to study the cell responses. The magnified images of cell morphology at three different positions (I, II, and III) are illustrated at the bottom of Fig. 3. The cell morphology before the heating treatment (0 h) is also given for comparison. It is seen at the beginning of the channel (0∼3800 μm, 60 °C to 51 °C) that the cytoplasm has collapsed and the nuclei appear to have swelled as shown in position I. The cells have indistinct boundaries. During the heating period, membrane blebs were detected around 25 min after the onset of the heating, then the cell cytoplasm suddenly collapsed (Fig. 4). Downstream to 3800 μm ∼8000 μm, 51 °C ∼43 °C, the cells still showed a necrotic morphology change but some cells shrank and became sequestered from each other (position II). The cell boundary looked much clearer than the upstream cells. The mechanism behind this slight difference should be addressed in future studies by more frequent tracking after the heating treatment. Beyond 8000 μm, e.g., position III, the cells appear rounder which could be a sign of early apoptosis.[31,32] Further downstream between from 9000 μm and 18 500 μm (about 42 °C down to 31.6 °C), a great portion of the cells are estimated to detach after comparing with the map before the heating (Fig. 3(b)). Worthy to note is that detachments were also detected in the non-hyperthermic zone where the temperature was lower than 37 °C. Finally, near the outlet reservoir, where temperature was around room temperature during the heating treatment, there was a very short area (from ∼18 500 μm to the outlet, below 32 °C) where the cells were alive and grew well. The distribution of cell amount along the channel is given in Fig. 5(a). The amount of the detached cells is represented by the light gray bar and it is seen that the detachment mostly occurred from 9000 to 16 000 μm, corresponding to the temperatures ranging from 42 to 34 °C. Figure 5(b) shows the percentage of cell detachment versus temperature along the channel (statistical result over 5 experimental trials).

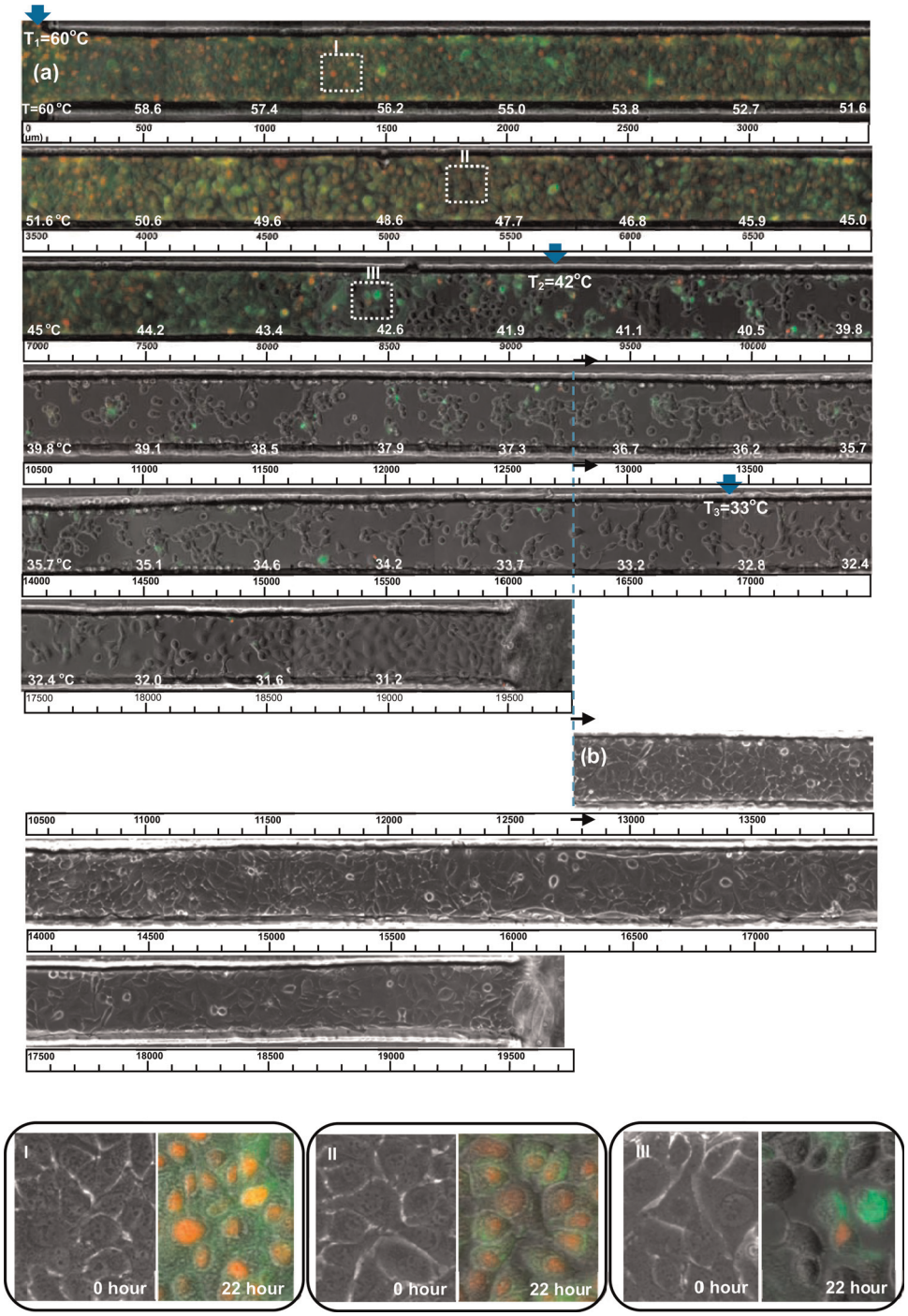

FIG. 3. (a) Map of cell damage stained by dual fluorescent dyes. Due to the confinement of the microscopy view field, a seamless connection for images has been conducted. The CaSki cells were heat-treated from 60 °C to 30 °C for around 105 min followed by incubation at 37 °C for around 22 h. Necrotic damage, apoptosis at different stages, and detachment and living cells were observed in sequence along the channel. Three positions I, II, and III were dotted circled in (a) and the magnified images of cell morphology change from 0 h to 22 h were given. (b) Cell morphology map before heating in the position where the temperature was below 37 °C during heating.

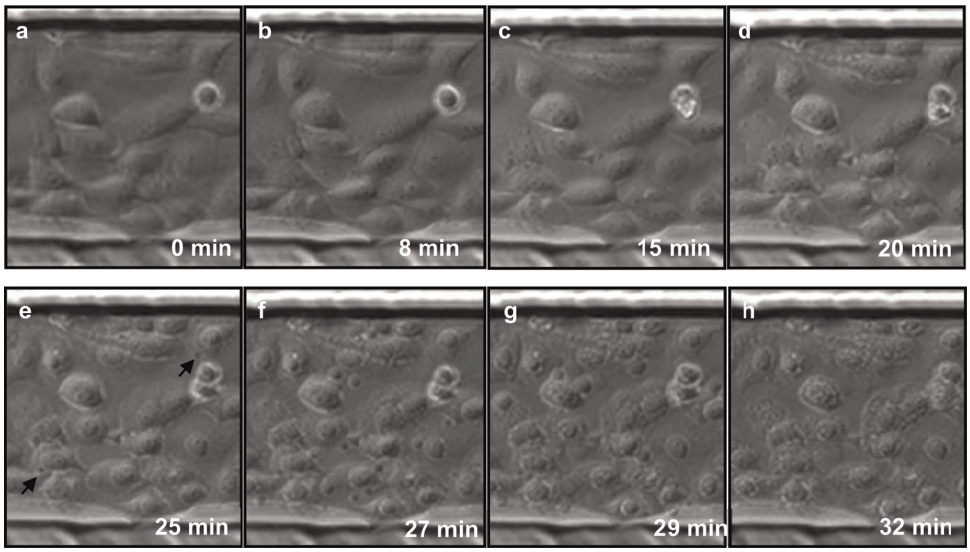

FIG. 4. Real time images for the cell morphology change during the heating. The cells expanded in size (b) and the nucleus swelled (c) and (d) in the first few minutes after applying heat. Then, necrotic blebs occurred near the plasma membrane (arrowed in (e)) and bloomed around the cell ((f) and (g)). The blebs grew quickly in size and then disappeared and the cells collapsed (h)).

Based on the above mapping of florescent staining and morphology imaging, it is expected that high temperatures (>45 °C) induce necrosis or late-stage apoptosis to the tumor cells, while mild hyperthermia (from 45 °C to 42 °C) mainly causes apoptosis at different stages. Heat shocks with the temperature below 42 °C are likely to trigger cell detachment. It is interesting to note that cell detachment also expanded into the non-hyperthermic zone (≤37 °C).

C. Cell detachment in hyperthermic zones

As shown in Fig. 3, cell detachment occurred in the hyperthermic zone from ∼9000 μm to ∼12 750 μm around 22 h post heating, corresponding to a temperature range between ∼42 °C and ∼37 °C. The adherent cells in this detachment zone were not stained using an apoptosis kit (Annexin V-FITC&PI), but they were rounder and seemed to detach from the substrate, which indicates they might undergo early apoptosis. Further tracking (42 h) at the location around 9100 μm (∼42 °C) revealed that some of the circular cells did detach from the bottom substrate (detached cells are marked by dotted arrows in Fig. 6(d)). As shown by the photographs taken at 90 h post heating (Fig. 6(e)), the cells swelled and shrank in size, but still attached to the monolayer.

D. Cell detachment in non-hyperthermic zones

Cell detachment was also detected in the zone where the temperature was equal or below 37 °C (around 12 750 μm from the inlet). Fig. 3(a), which was taken 22 h post heating, clearly shows that the cell population downstream in the channel was significantly less than that before the heating (Fig. 3(b)).

Vuento *et al.*[29] have studied the denaturation of fibronectin and found that this adhesion-mediating protein remains unchanged up to 55 °C, which is much higher than 37 °C. Therefore, the detachment in the non-hyperthermic zone cannot be due to the denaturation of the extracellular matrix. Fig. 7 shows the cell detachment in the region near $T_3 = 33$ °C after culturing the cells for 22, 42, and 90 h, respectively, following heating.

Cell detachment is one of the cellular responses in hyperthermic treatment[33–37] and the mechanisms associated with it have been studied extensively.[12,37–39] Vidair and Dewey[12] found cell detachment in Chinese hamster ovary cells (CHOs) several days after heating them for periods of 20 min or 30 min at 45 °C. They suggest that the acidification of the culture medium

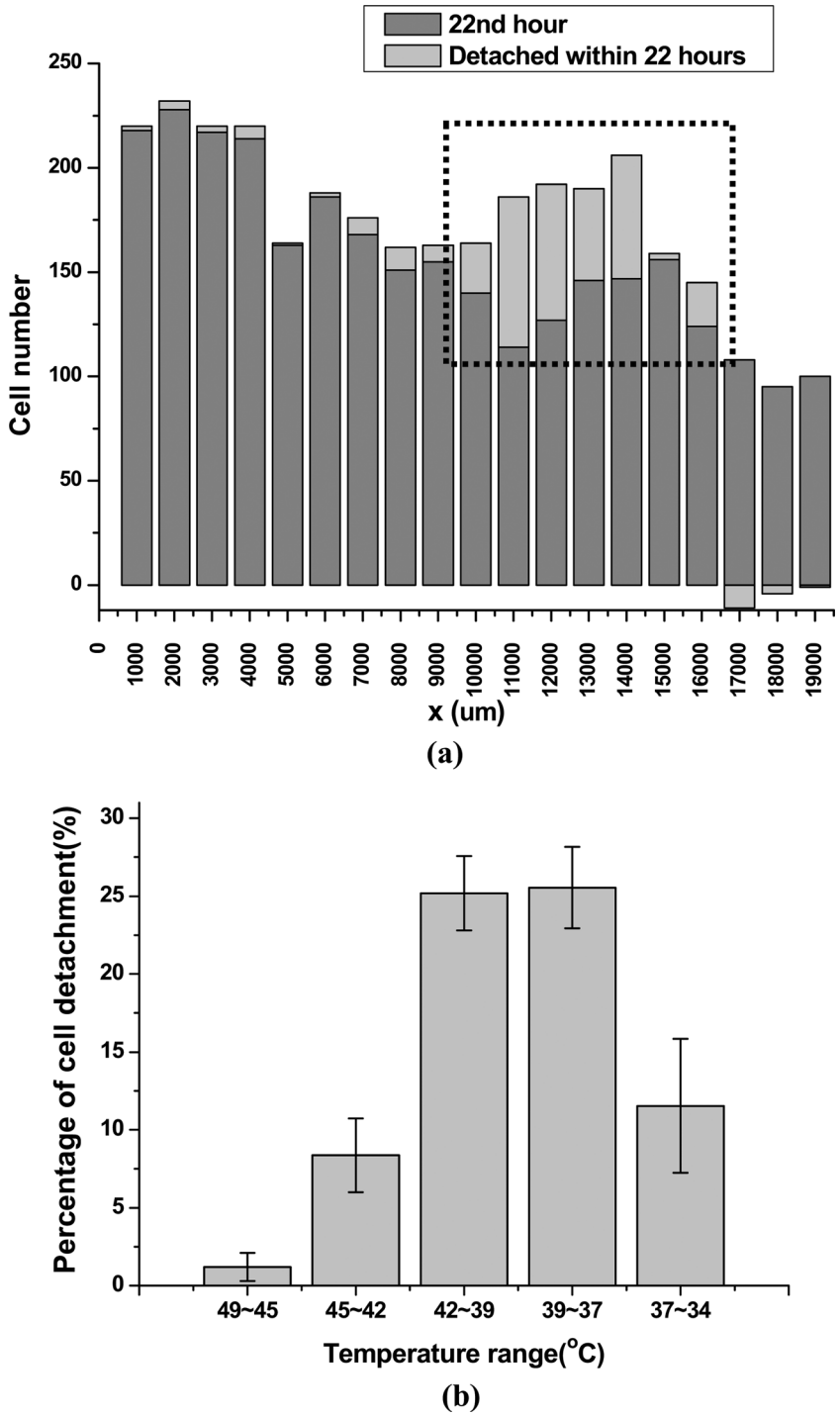

FIG. 5. The distribution of the cell amount along the channel at the 22nd h post heating (gray bar) and the detached cells within the 22 h (light gray bar) (a), and the cell detachment percentage versus the temperature along the channel (b).

might be a possible reason of the observed detachment. Wahl *et al.*[39] detected that acutely acidified cells (acute changes in the extracellular pH from 7.3 to 6.7 before onset of the heating) showed detachment from the substrate after hyperthermic treatment at 42 °C. The undetached cells were becoming rounder and more easily detached with a medium change. In another study,[38] the cytoskeletal protein alteration or loss on the plasma membrane was found to affect the cell adhesion to the substrate during hyperthermia-induced apoptosis, which results

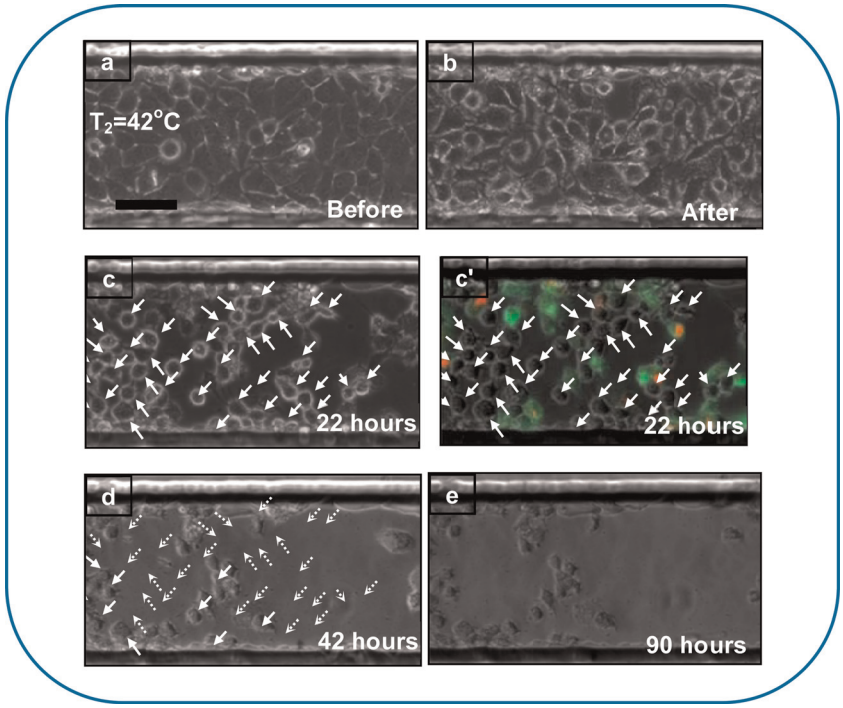

FIG. 6. Cell morphological changes at the position 9000 ~9400 μm before (a), right after (b), 22 h (c) and (c'), 42 h (d), and 90 h (e) after hyperthermic treatment. Rounding cells at 22 h were marked by arrows in (c) and (c'); detached cells at 42 h are marked by dotted arrows in (d) in order to make comparisons with (c). Cell detachment was observed at 22 h and 42 h post heating. The scale bar represents 100 μm.

in cell rounding/blebbing or anoikis. However, few studies have investigated the mechanisms of cell detachment below 37 °C by heating nearby cells. A recently published study[37] found that incubating the carcinoma cells (SK-OV-3) with the heat-shocked mesenchymal stem cells (MSCs) could cause significant tumor cell death. It was observed that the secreted factors from the heated MSCs induce cytoskeleton destruction and floating of the adherent tumor cells. The contents released from the heated MSCs might also markedly weaken the tumor cell progression by reducing the expression of antiapoptotic protein Bfl-1.

Our study demonstrates that the heated tumor cells and non-heated tumor cells interact in a microfluidic environment with a regional or selected hyperthermic treatment of some of the cells. It is no doubt that the vigorous cell detachment in the non-hyperthermic zone is the result of the upstream hyperthermic zone. The authors had conducted more than 10 experimental trials and the results are similar, i.e., the distributions of the death along the channels are similar, and the interaction between the heated and the non-heated cells are similar.

The current work did not include biological assays for analyzing the mechanisms of detachment in non-hyperthermic zones. The authors tried to measure the pH value of the fluid in the microchannel, finding that the volume of the fluid was too limited (about 0.2 μl) to have accurate pH measurement with traditional methods. Micro-sensor might be employed for accurate measurement.[40,41] Future experiments will be designed and conducted soon to analyze in more detail the effect of hyperthermic or non-hyperthermic zones on cellular damage rates.

E. Cell spreading downstream

Downstream and near the outlet, some cells are observed to spread on the substrate, as shown in Fig. 7(d) (42 h). The enlarged part of one cell exhibits significant spreading, which may indicate an early stage of adhesion. In Fig. 7(e) (90 h), some cells already have a polarized shape on the substrate but the proliferation is still inhibited. By phase contrast mapping at 90 h (data not shown), cell spreading occurs at a distance ~11 000 μm from the inlet, where the corresponding temperature is lower than 39 °C.

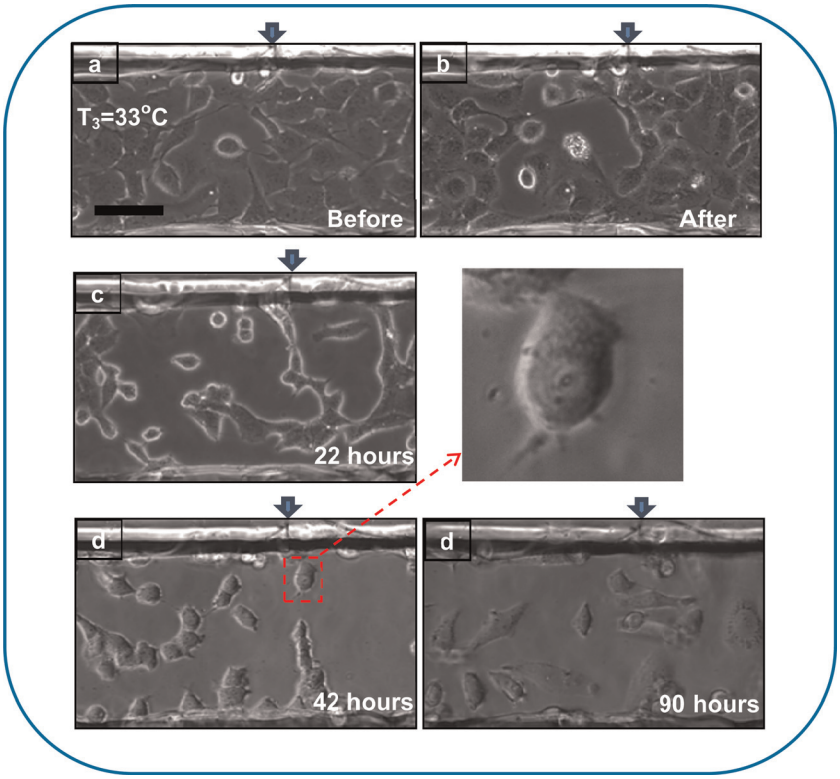

FIG. 7. Phase contrast images of cell morphological changes at the position, 16 650∼17 050 μm before (a) and right after (b) hyperthermic treatment; after 22 h (c), after 42 h (d), and after 90 h (e). The insert is an enlarged look of a radial spreading cell at 42 h post heating. Cell detachment was observed. Spreading cells and polarized cells were recorded in (d) and (e), respectively. The scale bar represents 100 μm.

IV. CONCLUSIONS

We have considered the hyperthermic cell death of CaSki cells in a microchannel in a PDMS microchip integrated with a directional heating scheme. A three dimensional (3D) numerical model was conducted for the heat transfer simulation, based on which a simple fitting method was proposed to easily estimate the temperature distribution along the channel. Hyperthermic ($>37\,^{\circ}$C) and non-hyperthermic ($\leq 37\,^{\circ}$C) zones were both achieved. Cell death along the channel, from high ($\sim 60\,^{\circ}$C) to low ($\sim 30\,^{\circ}$C) temperatures, was mapped at 22 h post heating by fluorescent dyes and tracked by phase contrast microscope for several days.

Necrotic cells, apoptotic cells at different stages, detached cells, and living cells were distinguished by dual fluorescent labeling and recorded in sequence along the channel. Cell detachment was observed in both the hyperthermic ($>37\,^{\circ}$C) and non-hyperthermic ($\leq 37\,^{\circ}$C) zones. By tracking the cells after incubating for 90 h, cell spreading was observed downstream in the channel where the heating temperature was lower than 39 °C. The present work not only gives a vivid map of cell responses under a temperature gradient but also reveals the potential interactions of heated tumor cells and non-heated tumor cells, which are seldom investigated in conventional petri-dish experiments.

ACKNOWLEDGMENTS

This work was supported by the National Natural Science Foundation of China (Grant No. 50876001). The authors thank the Lab of Phase Change and Interfacial Phenomena at Tsinghua University for their help throughout the work. The authors also thank Dr. Adriana Setchi at Imperial College London for the English editing.

[1]J. Bull, Cancer Res. **44**(10 Supplement), 4853 (1984).
[2]T. S. Hauck, T. L. Jennings, T. Yatsenko, J. C. Kumaradas, and W. C. W. Chan, Adv. Mater. **20**(20), 3832 (2008).
[3]R. S. Scott, R. J. R. Johnson, K. V. Story, and L. Clay, Int. J. Radiat. Oncol., Biol. Phys. **10**(11), 2119 (1984).
[4]A. Ito, F. Matsuoka, H. Honda, and T. Kobayashi, Cancer Gene Ther. **10**(12), 918 (2003).
[5]R. Gordon, J. Hines, and D. Gordon, Med.Hypotheses **5**(1), 83 (1979).
[6]A. Wagner, H. Weber, L. Jonas, H. Nizze, M. Strowski, F. Fiedler, H. Printz, H. Steffen, and B. Goke, Gastroenterology **111**(5), 1333 (1996).
[7]J. Moroi, S. Kashiwagi, S. Kim, M. Urakawa, H. Ito, and K. Yamaguchi, Int. J.Hyperthermia **12**(3), 345 (1996).
[8]S. Bhowmick, J. Coad, D. Swanlund, and J. Bischof, Int. J.Hyperthermia **20**(1), 73 (2004).
[9]K. Henle and D. Leeper, Radiat. Res. **66**(3), 505 (1976).
[10]B. Hildebrandt, P. Wust, O. Ahlers, A. Dieing, G. Sreenivasa, T. Kerner, R. Felix, and H. Riess, Crit. Rev. Oncol. Hematol. **43**(1), 33 (2002).
[11]Y. Rabin, Int. J. Hyperthermia **18**(3), 194 (2002).
[12]C. A. Vidair and W. C. Dewey, Radiat. Res. **116**(1), 157 (1988).
[13]J. L. Roti Roti, Int. J. Hyperthermia **24**(1), 3 (2008).
[14]Y. G. Shellman, W. R. Howe, L. A. Miller, N. B. Goldstein, T. R. Pacheco, R. L. Mahajan, S. M. LaRue, and D. A. Norris, J. Invest. Dermatol. **128**(4), 949 (2007).
[15]B. Harmon, A. Corder, R. Collins, G. Gobe, J. Allen, D. Allan, and J. Kerr, Int. J. Radiat. Biol. **58**(5), 845 (1990).
[16]H. M. Beere, J. Cell Sci. **117**(13), 2641 (2004).
[17]A. Ito, H. Honda, and T. Kobayashi, Cancer Immunol. Immunother. **55**(3), 320 (2006).
[18]A. Samali and T. G. Cotter, Exp. Cell Res. **223**(1), 163 (1996).
[19]X. He and J. C. Bischof, Ann. Biomed. Eng. **33**(4), 502 (2005).
[20]N. Crews, C. Wittwer, R. Palais, and B. Gale, Lab Chip **8**(6), 919 (2008).
[21]H. Mao, T. Yang, and P. S. Cremer, J. Am. Chem. Soc. **124**(16), 4432 (2002).
[22]C. Zhang and D. Xing, Nucl. Acids Res. **35**(13), 4223 (2007).
[23]S. K. Das, S. Chung, I. Zervantonakis, J. Atnafu, and R. D. Kamm, Biomicrofluidics **2**, 034106 (2008).
[24]E. M. Lucchetta, J. H. Lee, L. A. Fu, N. H. Patel, and R. F. Ismagilov, Nature **434**(7037), 1134 (2005).
[25]D. C. Duffy, J. C. McDonald, O. J. A. Schueller, and G. M. Whitesides, Anal. Chem. **70**(23), 4974 (1998).
[26]F. Wang, H. Wang, J. Wang, H. Y. Wang, P. L. Rummel, S. V. Garimella, and C. Lu, Biotechnol. Bioeng. **100**(1), 150 (2008).
[27]Y. Li, F. Wang, and H. Wang, Biomicrofluidics **4**, 014111 (2010).
[28]M. Franckena, L. J. A. Stalpers, P. Koper, R. G. J. Wiggenraad, W. J. Hoogenraad, J. D. P. van Dijk, C. C. Warlam-Rodenhuis, J. J. Jobsen, G. C. van Rhoon, and J. van der Zee, Int. J. Radiat. Oncol., Biol., Phys. **70**(4), 1176 (2008).
[29]M. Vuento, E. Salonen, K. Salminen, M. Pasanen, and U. Stenman, Biochem. J. **191**(3), 719 (1980).
[30]S. M. Yang and W. Q. Tao, *Heat Transfer*, 4th ed. (High Education Publisher, Beijing, China, 2006).
[31]M. B. Friis, C. R. Friborg, L. Schneider, M. B. Nielsen, I. H. Lambert, S. T. Christensen, and E. K. Hoffmann, J. Physiol. **567**(2), 427 (2005).
[32]G. Nagy, G. Pinter, G. Kohut, A. L. Adam, G. Trencsenyi, L. Hornok, and G. Banfalvi, DNA Cell Biol. **29**(5), 249 (2010).
[33]A. Gilmore, Cell Death Differ **12**, 1473 (2005).
[34]W. X. Li, C. Chen, C. Ling, and G. C. Li, Radiat. Res. **145**(3), 324 (1996).
[35]P. Ross-Riveros and J. T. Leith, Radiat. Res. **78**(2), 296 (1979).
[36]Y. J. Lee, J. H. Kim, S. Ryu, S. H. Kim, C. A. Vidair, E. P. Armour, and P. M. Corry, J. Thermal Biol. **19**(5), 305 (1994).
[37]J. A. Cho, H. Park, H. K. Kim, E. H. Lim, S. W. Seo, J. S. Choi, and K. W. Lee, Cancer **115**(2), 311 (2009).
[38]F. Luchetti, F. Mannello, B. Canonico, M. Battistelli, S. Burattini, E. Falcieri, and S. Papa, Apoptosis **9**(5), 635 (2004).
[39]M. L. Wahl, S. B. Bobyock, D. B. Leeper, and C. S. Owen, Int. J. Radiat. Oncol., Biol., Phys. **39**(1), 205 (1997).
[40]I. A. Ges, B. L. Ivanov, D. Schaffer, E. A. Lima, A. A. Werdich, and F. J. Baudenbacher, Biosens. Bioelectron. **21**(2), 248 (2005).
[41]S. E. Eklund, D. Taylor, E. Kozlov, A. Prokop, and D. E. Cliffel, Anal. Chem. **76**, 519 (2004).